

Laboratory experiment at 180.0° backscattering angle: lidar PDR dependency on refractive index and size across several aerosol types: mineral dust, pollen, soot.

Alain Miffre and Patrick Rairoux

Université Claude Bernard Lyon 1, CNRS, Institut Lumière Matière, UMR 5306, F-69100, Villeurbanne, France
alain.miffre@univ-lyon1.fr

Abstract: In polarization lidar experiments, the lidar particle depolarization ratio (*PDR*) is a key quantity, that typically hovers around 30 % for mineral dust, particularly in proximity to the source areas. To explore how the lidar *PDR* relates to the size and complex refractive index (*CRI*) of particles, a groundbreaking laboratory experiment (world first) was conducted for the first time at lidar exact backscattering angle of 180.0°, as reported by Miffre et al. in 2023 [1] at (355, 532) nm lidar wavelengths. Four dust samples differing in their *CRI* were investigated: silica (SiO₂), a major component of mineral dust, hematite, as the main light absorbent in mineral dust, then Arizona and Asian dust, two heterogeneous mixtures of the above two oxides in various proportions. At 355 nm, the lidar-measured *PDR* for silica was found equal to (33 ± 1) %. However, for hematite, the observed *PDR* was much lower, at only (10 ± 1) %. We hence demonstrate that when hematite is present, the complex refractive index governs the dust lidar *PDR*. In turn, Arizona dust exhibits higher depolarization than Asian dust, due to the higher proportion in hematite in the latter. Conversely, when hematite is less prevalent or absent, the dust lidar *PDR* is mostly size-dependent and increases with larger particle sizes, although the particle shape may also contribute to this trend. Moreover, similar laboratory findings were observed regarding six pollen types [2], namely ragweed, birch, pine, ash, spruce and cypress, and also soot [3] aerosols, which also exhibit light absorption properties at the 355 nm wavelength. We believe these laboratory findings, emphasizing the key role play the imaginary part of the complex refractive index, may help the lidar community to better interpret lidar inversions based on mineral dust, pollen and soot aerosols.

1. Introduction

Mineral dust, pollen and soot aerosols are highly important constituents of the atmosphere, with a multitude of impacts, for example on the Earth's radiative budget [4]. This impact is however difficult to quantify mainly due to the complexity in size, shape and composition of these particles, which prevents from quantifying light scattering by mineral dust as an analytical solution to Maxwell's equations. Moreover, in the atmosphere, these aerosols are additionally often mixed with other aerosols. To face such a complexity and discern the contribution of mineral dust in these particles mixture, ground-based and satellite-based polarization lidar instruments have been developed [5-8] relying on powerful partitioning algorithms have been developed [9]. Polarization lidar measurements on pollen [10-12] and smoke [9,12] have likewise been

developed. However, such lidar-based aerosol retrievals are under-constrained. Indeed, these algorithms rely on the priori knowledge of the intrinsic particles depolarization ratio (*PDR*) of these aerosols, which is a complex function of the particles size, shape and complex refractive index (*CRI*). Mineral dust, pollen and soot particles are indeed complex-shaped particles, which are difficult to model mathematically. Hence, light scattering numerical simulations cannot provide the lidar *PDR* accurately as they rely on simplifying assumptions regarding the complexity in shape of the particles. This is especially true for highly irregular-shaped mineral dust, but also for soot-fractal aggregates and pollen, as the latter exhibits a very complex shape, sometimes with spikes, holes and apertures. In turn, polarization lidar measurements on mineral dust [5-9], pollen [10-12] and smoke [9,12] are difficult to

interpret, mainly due to the particles complexity.

In this context, accurate measurements of the intrinsic lidar *PDR* of mineral dust, pollen and soot particles are highly coveted. Aerosol laboratory experiments at exact backscattering angle of 180.0° are hence highly desirable. Indeed, in the laboratory, the retrieved lidar *PDR* is, by construction, that of pure particles. Also, the dependence of the lidar *PDR* with size and complex refractive index can then be further discussed. However, in the literature, existing laboratory light scattering experiments only operate at scattering angles differing from the lidar backscattering angle of 180.0° and, also, at wavelengths differing from (355, 532) nm lidar wavelengths, while we learnt from Raman lidar signals how spectral corrections are important. This contribution reports on the findings of three recent publications [1-3], operating the only existing laboratory experiment at 180.0° lidar backscattering angle, at (355, 532) nm wavelengths to explore the dependence of the lidar *PDR* with size and complex refractive index. More precisely, the lidar *PDR* of the following samples are considered:

1. Mineral dust samples (silica, hematite, Arizona dust, Asian dust), differing in size and complex refractive index [1],
2. Pollen samples, differing in type (ragweed, birch, pine, ash, spruce and cypress) and then in size [2],
3. Soot particles, freshly-emitted from a pool fire [3].

Interestingly, these three separate publications [1-3] arrived to the same following conclusion: a higher imaginary part of the complex refractive index (*CRI*) decreases the lidar *PDR*. We believe these laboratory findings may help the lidar community to better interpret lidar inversions based on mineral dust, pollen and soot particles.

2. Laboratory experiment at 180.0°

Figure 1 schemes the aerosol laboratory experiment at exact lidar backscattering angle of 180.0° (world first, [1]). As in polarization lidar applications, this laboratory experiment relies on a ns-pulsed laser source at (355, 532) wavelengths and a polarization detector, noticeably involving a polarizing beam-splitter cube. Special care has been taken to ensure that

the lidar backscattering angle is covered with accuracy $(180.0 \pm 0.2)^\circ$ through a very precise alignment (1 mm out of 10 meters). The lidar *PDR* is accurately evaluated at (355, 532) nm wavelength simultaneously, after minimizing polarization and wavelength cross-talks.

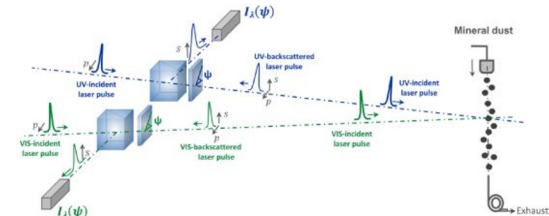


Figure 1. Laboratory experiment at lidar exact backscattering angle of 180.0° [1], allowing accurate retrievals of the lidar *PDR* at wavelengths 355 and 532 nm simultaneously.

This experiment relies on the scattering matrix formalism and details of its operation are given in [1]. In a few words, the detected backscattered intensity at wavelength λ is :

$$I_\lambda(\psi) = I_{0,\lambda} [a_\lambda - b_\lambda \cos(4\psi)] \quad (1)$$

where $I_{0,\lambda}$ depends on the power density of the laser, ψ is the rotation angle of a quarter wave-plate and coefficients a_λ and b_λ , only depend on the scattering matrix elements $F_{11,\lambda}$ and $F_{22,\lambda}$. The lidar *PDR* can then be accurately evaluated at wavelength λ by adjusting the experimental data points with Eq. (1) to get $I_{0,\lambda}a_\lambda$ and $I_{0,\lambda}b_\lambda$, then the ratio b_λ/a_λ . As developed in [1], this ratio relates to the lidar *PDR* at wavelength λ as follows $PDR_\lambda = (1 - b_\lambda/a_\lambda)/2$. Our laboratory findings are presented in Section 3 (for mineral dust), in Section 4 (for pollen types) and in Section 5 (for freshly-emitted soot particles). For the sake of clarity, Table 1 summarizes our main laboratory findings.

Table 1. Laboratory measurements of aerosol lidar *PDR* at 180.0° [1-3].

Aerosol	355 nm-PDR	532 nm-PDR
Silica	(33 ± 1)	(24 ± 1)
Hematite	(10 ± 1)	(17 ± 1)
Ragweed	(5 ± 1)	(33 ± 1)
Birch	(4 ± 1)	(31 ± 1)
Soot	(9 ± 2)	(12 ± 2)

While hematite efficiently absorbs light, especially at 355 nm wavelength, the hematite lidar *PDR* is lower than the silica lidar *PDR*. Likewise, ragweed, birch and soot particles are

efficient light absorbers at 355 nm wavelength and their lidar *PDR* is low in the range of 10 %. At 532 nm wavelength, at which silica, ragweed and birch practically do not absorb light, their lidar *PDR* is much more higher, in the range of 30 %. Still, hematite and soot, which are still light absorbers at this wavelength, exhibit a fairly lower lidar *PDR*.

3. Laboratory mineral dust *PDR* [1]

Using the methodology described in Section 2, we measured in laboratory the lidar *PDR* of silica, hematite, Arizona dust, and Asian dust. These samples were chosen as they exhibit distinct complex refractive indices. Hematite is indeed an efficient light absorber at wavelength 355 nm in contrary to silica. Arizona is rather silica-rich than Asian dust, the latter being rather hematite-rich, and hence a more efficient light absorber. To account for the size dependence of the lidar *PDR* these laboratory measurements were taken across two different size distributions (SD), referred to as "fine" and "coarse" in Table 2, which gathers our laboratory findings on mineral dust at wavelength 355 nm. When hematite is involved (as in the Asian dust sample), the lidar *PDR* slightly depends on the dust SD. When hematite is less (Arizona dust) or not involved (silica), the lidar *PDR* increases with increasing sizes, highlighting the importance of dual-wavelength polarization lidar measurements to address the involved particles sizes [7, 8,12].

To highlight the role of the imaginary part of the *CRI* on the lidar *PDR*, we also carefully measured the rutile lidar *PDR*. Indeed, the real part of rutile *CRI* is as large as that of hematite, but its imaginary part is negligible compared with hematite. The rutile lidar *PDR* was found to substantially differ from that of hematite. Our laboratory findings also agree with light scattering numerical simulations showing the high sensitivity of the lidar backscattering direction to particles inhomogeneity [13] and the lower dependence of scattering matrix elements on the particles shape when particles are efficient light absorbers [14]. While these numerical simulations rely on several assumptions, we here for the first time accurately quantify this behavior in laboratory. Moreover, in line with lidar applications, we partitioned the dust aerosol in its absorbing and non-absorbing components and showed that the dust aerosol *PDR* can then be retrieved as a

function of the fraction of hematite in the dust aerosol mixture, once accounted for the silica (absorbing) and hematite (non-absorbing) intrinsic lidar *PDR* [1].

Table 2. Laboratory measurements of 355 nm dust lidar *PDR* at 180.0° [1].

Aerosol	Fine SD	Coarse SD
Silica	(23 ± 1)	(33 ± 1)
Hematite	(11 ± 1)	(10 ± 1)
Arizona dust	(32 ± 1)	(34 ± 1)
Asian dust	(25 ± 1)	(25 ± 1)

4. Laboratory pollen *PDR* [2]

We likewise studied the laboratory *PDR* of several pollen types: ragweed, birch, pine, ash, spruce and cypress. Pollen are indeed important to study for allergenic health issues but also as a contributor to radiative transfer. Light backscattering by pollen cannot be numerically simulated since pollen are beyond the reach of numerically exact light scattering methods. As shown in Figure 3, from publication [2], the intrinsic lidar *PDR* of pure pollen is always lower at 355 nm wavelength compared with 532 nm wavelength, as highlighted also in Table 1.

Pure Pollen Particle Depolarization Ratio [%]

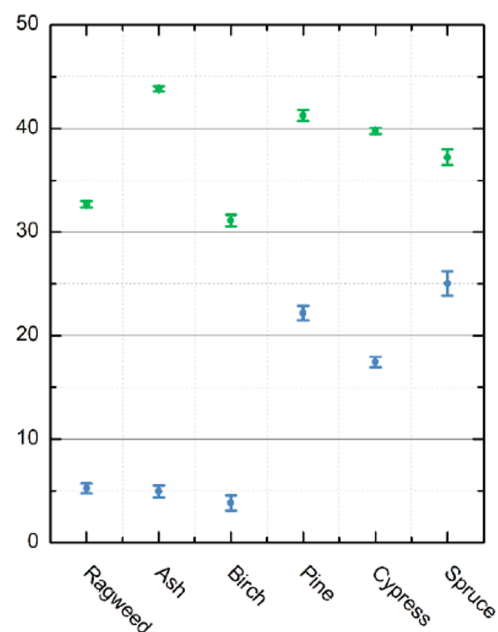


Figure 2. Lidar *PDR* of several pure pollen types at lidar exact backscattering angle of 180.0° [2], allowing accurate retrievals of the lidar *PDR* at wavelengths 355 and 532 nm.

5. Laboratory soot aerosol PDR [3]

Finally, the lidar *PDR* of freshly-emitted soot particles was measured in [3]. The aerosolization exhibited less stability in time compared with pollen, responsible for a larger error bar in the *PDR* retrievals. Nevertheless, within our experimental error bars, it however remained clear that the soot lidar *PDR* lies in the range of 10 % while soot particles absorb light at both 355 and 532 nm wavelengths.

6. Conclusion and outlooks

Dual-wavelength polarization lidars have become key in interpreting lidar measurements involving mineral dust [5-9], pollen [10-12] and soot [9,12] particles. Since these particles are mixed with other aerosols, such as spherical sulfates for mineral dust, partitioning algorithms have been developed [9], which are essential for retrieving the specific lidar backscattering coefficient of mineral dust, pollen and soot particles, but necessitates prior knowledge the intrinsic lidar *PDR* of these particles. The lidar *PDR* of pure particles is not accurately accessible in field where particles are mixed with other particles. Likewise, numerical simulations do not account for the real complexity in shape of the particles. To face such a complexity, we have developed a laboratory experiment, the only one to operate at lidar exact backscattering angle of 180.0° to accurately measure the aerosol lidar *PDR*. Two main laboratory findings can here be emphasized : i) the lidar *PDR* of mineral dust is not always close to 33 % as for silica, and may lower down to 10 % depending on the hematite fraction involved in the dust particles mixture. ii) The imaginary part of the complex refractive index (*CRI*) plays a key role in our laboratory *PDR*-measurements : whatever the aerosol type (dust, pollen, soot), the retrieved lidar *PDR* is lowered when considering wavelengths at which the considered aerosol is absorbing. We believe these laboratory findings are interesting for the lidar community, which measure these aerosols (dust, pollen, soot) every day, worldwide, by using dual-wavelength, or more, polarization lidar instruments. To interest a wide range of lidarists, the proposed oral presentation will start by recalling the benefits from polarization lidar measurements on mineral dust, pollen and smoke, before discussing on the above laboratory findings to

emphasize their benefit for the lidar community.

7. References

- [1] A. Miffre, D. Cholleton and P. Rairoux, "Visual system-response functions and estimating reflectance," *JOSA A* **14**, 741-755 (2023).
- [2] Cholleton, D., et al., *Rem. Sens.*, (2022).
- [3] Paulien, L., et al., *J. Quant. Spec. Rad. Transf.*, (2021).
- [4] IPCC, Climate Change 2021, *The Physical Science Basis*, Cambridge University Press, (2021).
- [5] Freudenthaler, V., et al., *Depolarization ratio profiling at several wavelengths in pure Saharan dust during SAMUM 2006*, *Tellus B* **61**, 165-179, (2009).
- [6] Hu, Q., et al., *The characterization fo Taklamakan dust properites using multi-wavelength polarization idar in Kashi, China*, *Atmos. Chem. Phys.* **20**, 13817-13834, (2020).
- [7] Haarig, M., et al., *First-triple wavelength lidar observations of depolarization and extinction-to-backscatter ratios of Saharan dust*, *Atmos. Chem. Phys.* **22**, 355-369, (2022).
- [8] Miffre, A., et al., *On the use of light polarization to investigate the size, shape and refractive index dependence of backscattering Angstroem exponents*, *Opt. Lett.*, **45**, 1084-1087, (2020).
- [9] Tesche, M., et al., *Vertically resolved separation of dust and smoke over Cape Verde using multiwavelength Raman and polarization lidars during Saharan dust experiment 2008*, *J. Geophys. Res.*, **114**, D13202, (2009).
- [10] Sicard, M. et al., *Measurement report: Characterization of the vertical distribution of airborne Pinus pollen in the atmosphere with lidar-derived profiles – a modelled case study in Barcelona*, *Atmos. Chem. Phys.* **21**, 17807-17832 (2021).
- [11] Figlioglu, et al., *Spectral dependence of birch and pine pollen optical properties using a synergy of lidar*, *Atmos. Chem. Phys.* **23**, 9009-9021, (a multi-wavelength, (2023).
- [12] Veselovskii, I., et al., *Retrieval and analysis of the composition of an aerosol mixture through Mie-Raman-Fluorescence lidar observations*, *Atmos. Meas. Tech. Discuss.*, in review, (2024).
- [13] Kahnert, M., *Modelling radiometric properties of inhomogeneous mineral dust particles*, *J. Quant. Spect. Rad. Transf.*, **152**; 16-27, (2015).
- [14] Mishchenko, M.I., et al., *Modeling phase functions for dustlike tropospheric aerosols using a shape mixture of randomly oriented polydisperse spheroids*, *J. Geophys. Res.*, **102**, 16831-16847, (1997).